Spin splitting and anisotropy of cyclotron resonance in the conduction band of GaAs

H. Mayer and U. Rössler
Institut für Theoretische Physik, Universität Regensburg, D-8400 Regensburg, Federal Republic of Germany
(Received 4 March 1991)

The recently observed spin splitting and anisotropy of cyclotron resonance in the conduction band of GaAs is quantitatively explained using a conduction-band Hamiltonian derived from a 14×14 $\mathbf{k}\cdot\mathbf{p}$ model together with an established parameter set. We thus demonstrate the importance of remote band contributions in the valence-band part of the Hamiltonian, which have been neglected so far.

I. INTRODUCTION

The anisotropy of the lowest conduction band in GaAs, which is obvious from an overview of the band structure throughout the first Brillouin zone, has been detected recently in a series of cyclotron-resonance (CR) experiments.[1–3] In particular, these experiments show the splitting of cyclotron-resonance transitions from the lowest ($N=0$) to the second ($N=1$) pair of spin-split Landau levels for magnetic fields $\mathbf{B}$ oriented parallel to the crystallographic [001], [111], and [110] directions (Fig. 1). These data were analyzed also with respect to the change of the mean resonance magnetic field relative to that obtained for the [001] direction (Fig. 2). An interpretation of these experimental results requires to extend the conduction-band model beyond the isotropic parabolic approximation, which is possible by considering contributions up to fourth order in the kinetic momentum operator $\mathbf{k}$ in the conduction-band Hamiltonian[4,5] or by calculating the conduction-band energies from a multilevel $\mathbf{k}\cdot\mathbf{p}$ Hamiltonian.[6–8] The former can be obtained from the latter in a systematic way by Löwdin perturbation theory.[5] Our calculations are based on a conduction-band Hamiltonian which is obtained from a 14×14 $\mathbf{k}\cdot\mathbf{p}$ model[5,7] by fourth-order perturbation theory using the computer algebra expert system MACSYMA.[9] It turns out that anisotropy of the conduction band results from $\mathbf{k}\cdot\mathbf{p}$ coupling between the p-bonding topmost valence-band and the p-antibonding conduction-band states (matrix element Q) but also from terms bilinear in $\mathbf{k}$, occuring in the valence-band part of the multiband Hamiltonian, due to second-order $\mathbf{k}\cdot\mathbf{p}$ coupling with remote bands. Pfeffer and Zawadzki[8] employ the so-called five-level $\mathbf{k}\cdot\mathbf{p}$ model,[10,11] using the same 14 basis states but without remote band contributions in the valence-band block and use the matrix element Q as fitting parameter. They succeeded in reproducing the observed spin splitting but failed to explain the anisotropy shift of the mean resonance magnetic field (dashed line in Fig. 2). In contrast, we take into account also the remote band contributions appearing in the valence-band block, use parameters which are well known from other experiments, and succeed in a quantitative interpretation of all these experimental data.

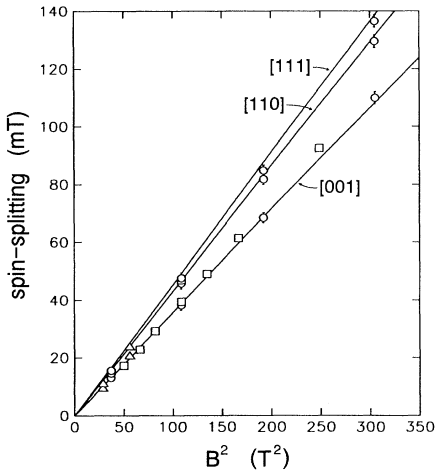

FIG. 1. Spin splittings of CR vs B^2 for the conduction electrons in GaAs for different field directions. Experimental results: ○, Sigg *et al.* (Ref. 2); □, Hopkins *et al.* (Ref. 3); △, Golubev *et al.* (Ref. 1). The solid lines are theoretical results calculated from our 2×2 model.

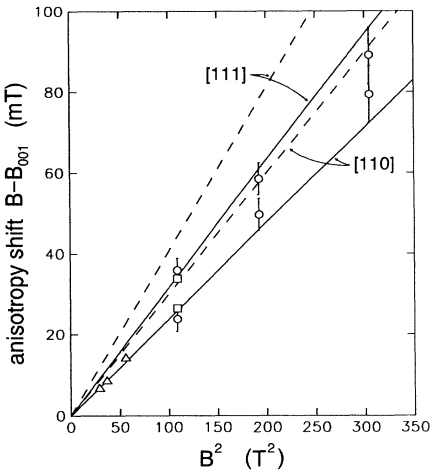

FIG. 2. Shift of the mean CR field relative to that in the [001] direction vs B^2 for the conduction electrons in GaAs for different field directions. Experimental results: ○, Sigg *et al.* (Ref. 2); □, Hopkins *et al.* (Ref. 3); △, Golubev *et al.* (Ref. 1). The solid curves are theoretical results calculated from our 2×2 model, the dashed lines are the results of Pfeffer and Zawadzki (Ref. 8).

II. THE k · p MODEL

In the presence of a magnetic field $\mathbf{B} = \nabla \times \mathbf{A}$ our initial Hamiltonian reads

$$H = \frac{\hbar^2 k^2}{2m} + V(\mathbf{r}) + \frac{\hbar^2}{4m^2c^2}(\boldsymbol{\sigma} \times \nabla V) \cdot \mathbf{k} - \tfrac{1}{2} g_0 \mu_B \boldsymbol{\sigma} \cdot \mathbf{B}, \tag{1}$$

where $\mathbf{k} = (\mathbf{p} + e\mathbf{A})/\hbar$ is the kinetic momentum operator, which satisfies the commutation relations $\mathbf{k} \times \mathbf{k} = (e/i\hbar)\mathbf{B}$, μ_B is the Bohr magneton, $g_0 = -2$ is the free-electron g factor, and $V(\mathbf{r})$ is the periodic crystal potential.

The 14×14 $\mathbf{k}\cdot\mathbf{p}$ model, which is discussed in this section, describes the p-bonding valence bands (Γ_{8v}, Γ_{7v}), the s-antibonding conduction band (Γ_{6c}), and the p-antibonding conduction bands (Γ_{8c}, Γ_{7c}), cf. Fig. 3. Due to the degeneracies within each of these five bands there are 14 quasidegenerate $\mathbf{k}\cdot\mathbf{p}$ basis states.

As a result of $\mathbf{k}\cdot\mathbf{p}$ theory and the Löwdin decoupling procedure we obtain a set of 14 coupled differential equations for 14 envelope functions $f_n(\mathbf{r})$. The $\mathbf{k}\cdot\mathbf{p}$ Hamiltonian $\underline{H}$ is the associated matrix differential operator acting on the 14-tupel of envelope functions. The 14×14 Hamiltonian falls into blocks with respect to the five bands under consideration:

$$\underline{H} = \begin{pmatrix} \underline{H}_{7v7v} & \underline{H}_{7v8v} & \underline{H}_{7v6c} & \underline{H}_{7v8c} & \underline{H}_{7v7c} \\ \underline{H}_{8v7v} & \underline{H}_{8v8v} & \underline{H}_{8v6c} & \underline{H}_{8v8c} & \underline{H}_{8v7c} \\ \underline{H}_{6c7v} & \underline{H}_{6c8v} & \underline{H}_{6c6c} & \underline{H}_{6c8c} & \underline{H}_{6c7c} \\ \underline{H}_{8c7v} & \underline{H}_{8c8v} & \underline{H}_{8c6c} & \underline{H}_{8c8c} & \underline{H}_{8c7c} \\ \underline{H}_{7c7v} & \underline{H}_{7c8v} & \underline{H}_{7c6c} & \underline{H}_{7c8c} & \underline{H}_{7c7c} \end{pmatrix}. \tag{2}$$

According to the generalized Wigner-Eckart theorem, which in this context is known as theory of invariants, each of these blocks may be formulated as a sum of invariants built as products of irreducible sets of basis matrices and of irreducible tensor components. From the comparison of this invariant expansion with the results of perturbation theory we obtain the Hamiltonian matrix of Table I, which is an extension of Table IV in Ref. 6.

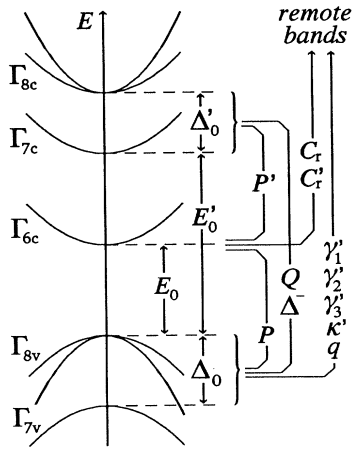

FIG. 3. Schematic band structure for the 14×14 model. Besides the energy separations at the Γ point (E_0, E_0', Δ_0, Δ_0') the couplings within the model are indicated, an explanation is given in the text.

Our model contains the following energy gaps and spin-orbit splittings:

$$E_0 = E(\Gamma_{6c}) - E(\Gamma_{8v}), \qquad E_0' = E(\Gamma_{7c}) - E(\Gamma_{8v}),$$
$$\Delta_0 = E(\Gamma_{8v}) - E(\Gamma_{7v}), \qquad \Delta_0' = E(\Gamma_{8c}) - E(\Gamma_{7c}).$$

We also include the inversion asymmetry induced off-diagonal spin-orbit coupling between the $\Gamma_{8v} + \Gamma_{7v}$ and $\Gamma_{8c} + \Gamma_{7c}$ states through the parameter Δ^-.[12] According to our phase convention the momentum matrix elements P between Γ_{6c} and $\Gamma_{8v} + \Gamma_{7v}$ states and Q between $\Gamma_{8v} + \Gamma_{7v}$ and $\Gamma_{8c} + \Gamma_{7c}$ states are real, the inversion asymmetry-induced parameters P' (momentum matrix element between Γ_{6c} and $\Gamma_{8c} + \Gamma_{7c}$ states) and Δ^- are purely imaginary.

The remote band contributions to the effective mass and effective g-factor tensors of the valence bands are taken into account through the reduced Luttinger parameters γ_1', γ_2', γ_3', κ', and q. These can be obtained from the Luttinger parameters γ_1^L, γ_2^L, γ_3^L, and κ^L by

$$\gamma_1' = \gamma_1^L - \frac{2}{3}\frac{m}{\hbar^2}\left(\frac{P^2}{E_0} + \frac{Q^2}{E_0' + \Delta_0'} + \frac{Q^2}{E_0'}\right), \tag{3}$$

$$\gamma_2' = \gamma_2^L - \frac{1}{3}\frac{m}{\hbar^2}\left(\frac{P^2}{E_0} - \frac{Q^2}{E_0'}\right), \tag{4}$$

$$\gamma_3' = \gamma_3^L - \frac{1}{3}\frac{m}{\hbar^2}\left(\frac{P^2}{E_0} + \frac{Q^2}{E_0'}\right), \tag{5}$$

$$\kappa' = \kappa^L - \frac{1}{3}\frac{m}{\hbar^2}\left(\frac{P^2}{E_0} - \frac{2}{3}\frac{Q^2}{E_0' + \Delta_0'} - \frac{1}{3}\frac{Q^2}{E_0'}\right) + \frac{1}{3}. \tag{6}$$

The reduction of the Luttinger parameters is necessary because we include the $\mathbf{k}\cdot\mathbf{p}$ couplings between the p-

TABLE I. Invariant expansion of the 14×14 Hamiltonian. For the definition of the block matrices T_α, U_α, cf. Ref. 6. $\mathbf{J}$ denotes the $j = \frac{3}{2}$ angular momentum matrices, σ the Pauli spin matrices. The symmetrized product is defined as $\{ab\} = \frac{1}{2}(ab + ba)$.

$$\begin{aligned}
\underline{H}_{7v7v} &= -\Delta_0 - (\hbar^2/2m)\gamma_1' k^2 - (2\kappa' - \tfrac{1}{6}g_0)\mu_B(\boldsymbol{\sigma}\cdot\mathbf{B}) \\
\underline{H}_{8v8v} &= -(\hbar^2/2m)\{\gamma_1' k^2 - 2\gamma_2'[(J_x^2 - \tfrac{1}{3}J^2)k_x^2 + \text{c.p.}] \\
&\qquad -4\gamma_3'[\{J_x J_y\}\{k_x k_y\} + \text{c.p.}]\} \\
&\qquad -\mu_B\{[(2\kappa' + \tfrac{1}{3}g_0)J_x + 2qJ_x^3]B_x + \text{c.p.}\} \\
\underline{H}_{6c6c} &= E_0 + (1 + C_r)(\hbar^2/2m)k^2 - \tfrac{1}{2}g_0(1 + C_r')\mu_B(\boldsymbol{\sigma}\cdot\mathbf{B}) \\
\underline{H}_{8c8c} &= E_0' \\
\underline{H}_{7c7c} &= E_0' + \Delta_0' \\
\underline{H}_{8v7v} &= (\hbar^2/2m)[6\gamma_2'(U_{xx}k_x^2 + \text{c.p.}) \\
&\qquad +12\gamma_3'(U_{xy}\{k_x k_y\} + \text{c.p.})] \\
&\qquad -\mu_B(3\kappa - g_0)(U_x B_x + \text{c.p.}) \\
\underline{H}_{6c7v} &= -(1/\sqrt{3})P\mathbf{k}\cdot\boldsymbol{\sigma} \\
\underline{H}_{8c7v} &= -2Q(U_{yz}k_x + \text{c.p.}) \\
\underline{H}_{7c7v} &= -\tfrac{2}{3}\Delta^- \\
\underline{H}_{6c8v} &= \sqrt{3}P(T_x k_x + \text{c.p.}) \\
\underline{H}_{8c8v} &= -\tfrac{2}{3}Q(\{J_y J_z\}k_x + \text{c.p.}) + \tfrac{1}{3}\Delta^- \\
\underline{H}_{7c8v} &= -2Q(T_{yz}k_x + \text{c.p.}) \\
\underline{H}_{8c6c} &= -\sqrt{3}P'(U_x k_x + \text{c.p.}) \\
\underline{H}_{7c6c} &= (1/\sqrt{3})P'\boldsymbol{\sigma}\cdot\mathbf{k} \\
\underline{H}_{7c8c} &= 0
\end{aligned}$$

bonding valence bands and the s- and p-antibonding conduction bands directly in our multiband model.

The explicit treatment of the off-diagonal spin-orbit coupling Δ^- requires also that the Hermann-Weisbuch parameters[11] C and C' are reduced to corresponding parameters C_r and C'_r by the resulting contributions to the electron effective mass and effective g factor:

$$C_r = C - \frac{8}{9}\frac{m}{\hbar^2}\Delta^- PP'\left(\frac{1}{E_0(E_0-E'_0-\Delta'_0)} - \frac{1}{(E_0+\Delta_0)(E_0-E'_0)}\right), \quad (7)$$

$$C'_r = C' + \frac{4}{9}\frac{m}{\hbar^2}\Delta^- PP'\left(\frac{1}{E_0(E_0-E'_0-\Delta'_0)} + \frac{2}{(E_0+\Delta_0)(E_0-E'_0)}\right). \quad (8)$$

In principle the structure of the p-antibonding conduction band blocks within our Hamiltonian should contain analogous terms to that weighted by the Luttinger parameters. Because there is as yet no indication that these terms are detectable in experiments, we consider their influence on the conduction-band states as being small enough to be neglected. The five-level $\mathbf{k}\cdot\mathbf{p}$ model of Refs. 8 and 10 is obtained by neglecting in Table I all remote band contributions in the valence-band block, i.e., by choosing $\gamma'_1 = -1$, $\gamma'_2 = \gamma'_3 = \kappa' = q = 0$.

III. CALCULATION OF LANDAU LEVELS

The standard procedure to calculate the Landau levels from a $\mathbf{k}\cdot\mathbf{p}$ Hamiltonian is to expand each of the envelope functions into harmonic-oscillator eigenfunctions and to diagonalize the resulting number matrix. This merely numerical treatment obscures the influence of the various couplings within the 14×14 model on the field dependence of the conduction-band Landau levels. In order to avoid this inconvenience and to give a systematic description of these dependencies we split the diagonalization of the 14×14 model into two steps by introducing an effective 2×2 conduction-band Hamiltonian $\mathcal{H}$ as an intermediate result. This Hamiltonian contains all resulting terms up to fourth order in $\mathbf{k}$ (i.e., second order in $\mathbf{B}$) and can be obtained from the 14×14 Hamiltonian by performing an algebraic block diagonalization (Löwdin partitioning). Its invariant expansion is well known (see Ref. 5, Sec. 2.1):

$$\mathcal{H} = \sum_{\kappa,\lambda} a_{\kappa,\lambda} \sum_{l} X_l^{(\lambda)} \mathcal{K}_l^{(\kappa,\lambda)}. \quad (9)$$

The block diagonalization yields formulas for the expansion coefficients $a_{\kappa,\lambda}$ in terms of the 14×14 model parameters. In contrast to previous work[5] the extensive algebra which is necessary for the block-diagonalization was carried out using the computer algebra expert system MACSYMA.[9,13]

The second step in our calculation of the Landau levels for the conduction electrons is the application of the standard procedure (see above) on the 2×2 Hamiltonian $\mathcal{H}$ with the expansion coefficients $a_{\kappa,\lambda}$, which are calculated from the 14×14 model parameters.

Our procedure to calculate conduction-band Landau levels from the 14×14 problem has the following advantage over the method used by Pfeffer and Zawadzki:[8] The expansion coefficients of the 2×2 Hamiltonian have clear physical interpretations which are closely related to the experimental CR spectra:[5] The weighting factor $a_{1,4}$ essentially determines the anisotropy of the effective mass, $a_{4,3}$ determines the field dependence of the g factor in the [001] direction, and $a_{4,5} - a_{4,4}$ determines the deviations of this field dependence for the other directions of the magnetic field relative to that for the [001] direction. Thus, using our 2×2 model allows us easily to distinguish between symmetry properties, which are identical for all zinc-blende-type semiconductors, and material specific properties, which is quite useful for the explanation of experimental data.

IV. RESULTS

The theory outlined in the preceding sections may be applied to any semiconductor with zinc-blende symmetry. For GaAs we use the parameter set of Table II.

From these parameters we determined the expansion coefficients $a_{\kappa,\lambda}$ of the 2×2 model for GaAs using the general expressions which we obtained through the algebraic block diagonalization of the 14×14 Hamiltonian. We expanded each of the conduction-band envelope functions into up to 16 harmonic-oscillator functions and diagonalized the resulting number matrix. The eigenvalues for a given orientation and strength of the magnetic field form a ladder of spin-split Landau levels. We determined the Landau levels for $\mathbf{B} \parallel [001]$, $\mathbf{B} \parallel [111]$, and $\mathbf{B} \parallel [110]$ as a function of the magnetic-field strength. This finally enabled us to give theoretical values for the shift in the mean resonance field with respect to that for the [001] direction and the spin splitting of the cyclotron resonance.

Figures 1 and 2 show that our results reproduce the experimental data. In particular, Fig. 2 demonstrates the importance of remote band contributions in the valence-band blocks of our 14×14 Hamiltonian, which were neglected by Pfeffer and Zawadzki. The agreement of our results with the experiments is much better than that of Pfeffer and Zawadzki, though they used the parameter Q to fit the experiments. This proves the reliability of our 14×14 model and of our parameter set.

TABLE II. Parameter set for GaAs, taken from Ref. 14 or calculated from the parameters therein.

$E_0 = 1.519$ eV	$\gamma_1^L = 6.85$	$C = -1.878$
$\Delta_0 = 0.341$ eV	$\gamma_2^L = 2.10$	$C' = -0.021$
$E'_0 = 4.488$ eV	$\gamma_3^L = 2.90$	$P = 10.493$ eV Å
$\Delta'_0 = 0.171$ eV	$\kappa^L = 1.20$	$P' = i4.780$ eV Å
$\Delta^- = -i0.050$ eV[a]	$q = 0.01$	$Q = 8.165$ eV Å

[a] Reference 2.

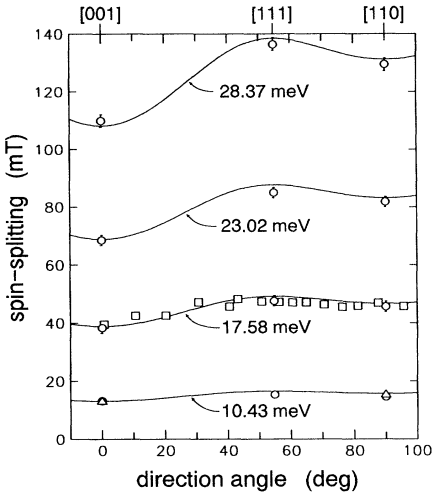

FIG. 4. Directional dependence of the spin-splitting of CR for the conduction electrons in GaAs for different transition energies. The angle θ determines the direction of the magnetic field in the $(1\bar{1}0)$ plane. Experimental results: ○, Sigg *et al.* (Ref. 2); □, Hopkins *et al.* (Ref. 3); △, Golubev *et al.* (Ref. 1). The solid lines are theoretical results calculated from our 2×2 model.

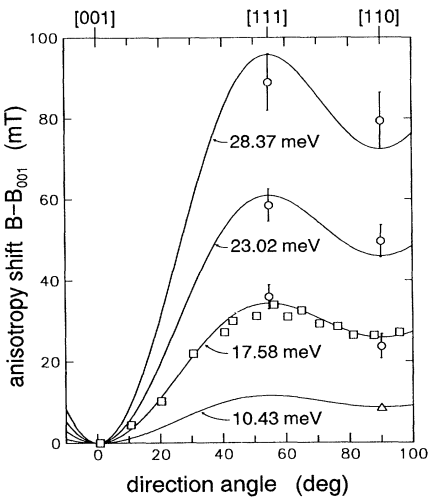

FIG. 5. Directional dependence of the shift in the mean CR field relative to that in the [001] direction for the conduction electrons in GaAs for different transition energies. The angle θ determines the direction of the magnetic field in the $(1\bar{1}0)$ plane. Experimental results: ○, Sigg *et al.* (Ref. 2); □, Hopkins *et al.* (Ref. 3); △, Golubev *et al.* (Ref. 1). The solid lines are theoretical results calculated from our 2×2 model.

We did not consider the magnetopolaron coupling in our calculations because its influence on the anisotropy of the cyclotron resonance is expected to be of higher order in B than the experimentally observed splittings.

As a further test for our theory we investigated the directional dependence of the anisotropy shift of the mean resonance field and that of the spin splitting for magnetic fields in the $(1\bar{1}0)$ plane. A comparison of our results with the experimental data of Sigg *et al.*,[2] Hopkins *et al.*,[3] and Golubev *et al.*[1] is shown in Figs. 4 and 5. The angle θ is defined as $\theta = \arccos(\hat{\mathbf{z}}\cdot\mathbf{B}/B)$, i.e., $\theta_{001} = 0°$, $\theta_{110} = 90°$, and $\theta_{111} = 54.73°$. Again we find a very good agreement with the experiments.

In conclusion, we present a model capable of describing quantitatively spin splitting and anisotropy of cyclotron resonance in the conduction band of zinc-blende semiconductors. The essential improvement over existing concepts is the inclusion of remote band contributions in the valence-band part of the 14×14 $\mathbf{k}\cdot\mathbf{p}$ Hamiltonian and the application of a computer algebra expert system for the Löwdin partitioning procedure, which allows us to consider also additional perturbations, e.g., by external stress, in a straightforward way. The strength of the model is demonstrated by a quantitative interpretation of experimental data for GaAs.

ACKNOWLEDGMENT

One of us (U.R.) benefited from frequent discussions with H. Sigg.

[1] V. G. Golubev, V. I. Ivanov-Omskii, I. G. Minervin, A. V. Osutin, and D. G. Polyakov, Zh. Eksp. Teor. Fiz. **88**, 2052 (1985) [Sov. Phys. JETP **61**, 1214 (1985)].

[2] H. Sigg, J. A. A. J. Perenboom, P. Pfeffer, and W. Zawadzki, Solid State Commun. **61**, 685 (1987).

[3] M. A. Hopkins, R. J. Nicholas, P. Pfeffer, W. Zawadzki, D. Gauthier, J. C. Portal, and M. A. di Forte-Poisson, Semicond. Sci. Technol. **2**, 568 (1987).

[4] N. R. Ogg, Proc. Phys. Soc. London **89**, 43 (1966).

[5] M. Braun and U. Rössler, J. Phys. C **18**, 3365 (1985).

[6] H.-R. Trebin, U. Rössler, and R. Ranvaud, Phys. Rev. B **20**, 686 (1979).

[7] U. Rössler, Solid State Commun. **49**, 943 (1984).

[8] P. Pfeffer and W. Zawadzki, Phys. Rev. B **41**, 1561 (1990).

[9] MACSYMA™, Massachusetts Institute of Technology (1982), Symbolics Inc., Cambridge, MA (1982, 1986); H. Mayer, Diploma thesis, Universität Regensburg, 1990.

[10] M. Cardona, J. Phys. Chem. Solids **24**, 1543 (1963).

[11] C. Hermann and C. Weisbuch, Phys. Rev. B **15**, 823 (1977).

[12] F. H. Pollak, C. W. Higginbotham, and M. Cardona, J. Phys. Soc. Jpn. Suppl. **21**, 20 (1966); M. Cardona, N. E. Christensen, and G. Fasol, Phys. Rev. B **38**, 1806 (1988).

[13] Up to terms connected with the last term of Eq. (1) and with Δ^- this procedure confirms the result of Ref. 5 except for a misprint in Table 3 therein, where the prefactor in the definition of δ_1^2 should read $-\frac{8}{3}$ instead of $-\frac{4}{3}$.

[14] *Semiconductors*, edited by O. Madelung, Landolt-Börnstein, New Series, Vol. 17a (Springer, Berlin, 1982), p. 128.